

# **GEOLOGIC MAP OF THE PHILUS SULCUS (Jg-4) QUADRANGLE OF GANYMEDE**

By Scott L. Murchie and James W. Head

1989

Prepared for the National Aeronautics and Space Administration  
by  
U.S. Department of the Interior, U.S. Geological Survey

(Published in hardcopy as USGS Miscellaneous Investigations Series Map I-1966, as part of the Atlas of Jovian Satellites, 1:5,000,000 Geologic Series. Hardcopy is available for sale from U.S. Geological Survey, Information Services, Box 25286, Federal Center, Denver, CO 80225)

Please direct questions or comments about the digital version to:

Richard Kozak  
U.S. Geological Survey  
2255 N. Gemini Drive  
Flagstaff, AZ 86001

e-mail: [rkozak@flagmail.wr.usgs.gov](mailto:rkozak@flagmail.wr.usgs.gov)

## DESCRIPTION OF MAP UNITS

### LIGHT MATERIALS

**Smooth material**—Intermediate to high albedo; geomorphically smooth at scale of Voyager resolution. Embays dark materials and some grooved materials. In places crosscut by grooves, groove pairs, and narrow groove lanes. *Interpretation:* Extrusive or possibly pyroclastic deposits of brine or brine-ice slurry having low silicate content; concentrated in topographic lows, especially downdropped blocks. Younger than some grooves but older than others

**Grooved material**—High albedo. Subdued to conspicuous grooves 40 km to several hundred kilometers long, commonly in parallel to subparallel sets with 5- to 50-km groove spacing. Individual grooves flat-floored to sinusoidal in cross section. Contacts with dark units commonly defined by diffuse-edged, intermediate-albedo, smooth materials. *Interpretation:* Groove sets are tectonic blocks of dark materials, downdropped and resurfaced by light smooth material, and subsequently fractured pervasively by narrow grabens, tension fractures, or both. Sinusoidal groove cross sections due in part to mass wasting

**Mottled grooved material**—Overall intermediate albedo, having lighter patches at scale of tens of kilometers. Occurs as polygons several hundred kilometers in size, locally surrounded and partly dissected by throughgoing grooves or groove pairs and narrow groove lanes. *Interpretation:* Thinly resurfaced dark material fractured by groove formation

### DARK MATERIALS

**Grooved material**—Forms two low-albedo, polygonal areas having grooves spaced 10 to 50 km apart. Surrounded by light smooth or grooved materials. No conspicuous furrows. *Interpretation:* Degraded dark furrowed material, fractured by same tectonic processes responsible for formation of light grooved material

**Lineated material**—Forms low- to intermediate-albedo, mottled areas between intersecting light-material bands. Irregular or sublinear to reticulate elongate depressions or albedo markings where observed at higher resolution. *Interpretation:* Dark furrowed material degraded by fracturing, mass wasting, or both

**Furrowed material**—Low-albedo material dissected by light-material bands to form polygons as much as thousands of kilometers in size. Most densely cratered material in area, and only material containing large number of degraded craters and palimpsests. Morphology dominated by furrows, which are sets of parallel to subparallel arcuate to linear troughs 6 to 10 km wide and several hundred meters deep. Patches 20 to 100 km across have lower albedo. *Interpretation:* Oldest unit, consisting of mixture of ice and silicate, possibly resurfaced before formation of observed morphology; darkened by radiation, meteoritic contamination, and ablation of ices. Fractured by tectonic and giant impact processes to form furrows

### CRATER MATERIALS

**Material of bright craters**—Forms sharp-rimmed craters of high relief, some containing central peaks or central pits, and high-albedo ejecta surrounding these craters; ejecta range from rays (youngest ejecta) to

diffuse-edged bright patches. More common in light than dark materials. Few patches of low-albedo ray material. *Interpretation:* Youngest impact craters; ejecta composed of frost-rich deposits. Dark patches may result from projectile contamination, low-albedo lag from devolatilized bright rays, or excavated dark material

**Material of partly degraded craters**—Forms floors, internal structures, rims, and ejecta of craters having sharp rims and high relief. Albedo similar to target material, but dark floors common in small craters in light terrain (such as at lat 22° N., long 187°). Traces of bright ejecta on some rims and floors. *Interpretation:* Impact craters and ejecta of intermediate age, affected by long-term ablation of volatiles, mass wasting, and impact gardening

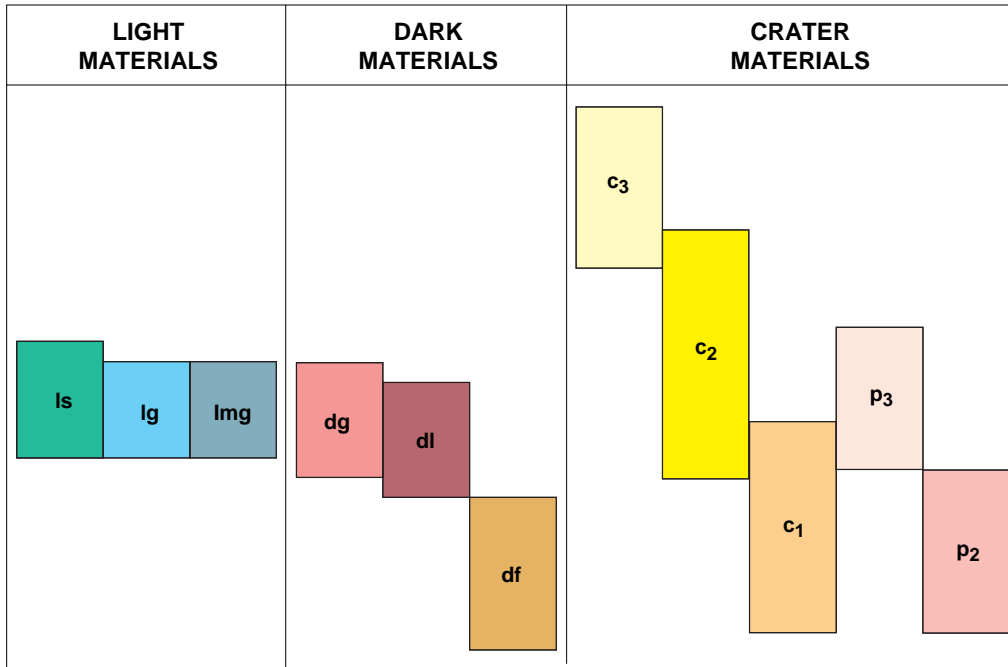
**Material of degraded craters**—Forms craters having flat floors and subdued but resolvable rims. Ejecta commonly unresolved or furrows resolvable nearly to rim, suggesting thin ejecta. Albedo same as dark target material. *Interpretation:* Impact craters generally predating light materials; degraded by ablation of volatiles, mass wasting, impact gardening, and probably viscous relaxation

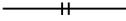
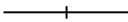
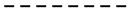
**Palimpsest materials**—Circular patches of intermediate to high albedo

**Material of basinlike palimpsest**—Hummocky, high-albedo surface with several low, concentric ridges and flatter central area. Surrounded by field of secondary craters. *Interpretation:* Impact basin whose high-relief features partly collapsed under own weight either immediately after impact because of low lithospheric strength or over time because of viscous relaxation

**Material of subdued palimpsests**—Low- to intermediate-albedo surfaces in dark materials. Geomorphically subdued, having barely resolvable, low, arcuate ridges arranged roughly concentrically to center of patch. No secondary craters. Furrows of dark materials partly buried, found only in outer parts. *Interpretation:* Ancient impact craters whose high-relief features collapsed under own weight. Central parts are degraded basins; outer parts are ejecta

### CORRELATION OF MAP UNITS



	<b>Contact</b> —Dashed where approximately located; dotted where buried. Includes boundaries between groove sets; these boundaries may terminate without closure
	<b>Graben or grabenlike structure</b> —Dotted where buried
	<b>Major furrow or dark-terrain trough</b>
	<b>Throughgoing conspicuous groove</b> —Commonly crosscuts or bounds groove domains
	<b>Trend of sharp groove set</b> —Schematic
	<b>Trend of subdued groove set</b> —Schematic
	<b>Albedo lineament or curvilineament</b>
	<b>Crater rim crest</b>
	<b>Subdued or buried crater rim crest</b>
	<b>Central peak</b>
	<b>Central pit</b> —Symbol outlines depression
	<b>Central dome</b>
	<b>Basin ring</b>
	<b>Palimpsest ring</b>
	<b>Bright crater rays</b>
	<b>Dark crater rays</b>
	<b>Secondary crater field</b>

## INTRODUCTION

The Philus Sulcus quadrangle is located in the anti-Jovian hemisphere of Ganymede, the third and largest of the Galilean satellites. The 180° meridian defining the quadrangle's east boundary passes through the anti-Jovian point at the equator, and the 270° meridian forming the quadrangle's west boundary crosses the trailing point in the satellite's orbit.

Ganymede consists of a mixture of rock and ice having an average density of 1.93 g/cm<sup>3</sup> (Smith and others, 1979a, b). The high albedo of the satellite's surface (40 to 60 percent) and absorption features in its spectrum suggest that water ice is the dominant surface material and that it is intermixed with at least several percent of silicates and minerals containing oxidized iron (Clark and others, 1986). The surface is about equally divided between light and dark materials whose albedos may differ as a result of slightly different silicate contents. Both materials contain craters ranging in morphology from fresh (sharp rims and bright rays) to degraded. Two types of tectonic structures are pervasive, furrows and grooves. Furrows are linear to arcuate troughs, commonly having raised rims, that occur solely in dark material. Large areas of dark material, most of which appear furrowed where seen at high resolution, are named regiones. Grooves are linear, U-shaped troughs that are strongly concentrated in light materials but also occur in dark materials; where they consistently crosscut the furrows. Bands of light grooved material are named sulci. Within the sulci, grooves occur most commonly in parallel to subparallel sets or domains having laterally continuous groove orientation and morphology, and they form large areas of grooved terrain. Two principal types of domains are represented in the Philus Sulcus area (Murchie and Head, 1985b). Groove lanes are elongate to linear and typically of light material; their grooves are parallel to the domains' long axes. Grooved polygons are blocky to polygonal in outline and of either light or dark material; their grooves trend at oblique angles to the domains' long axes.

## GENERAL GEOLOGY

The mapped units are material units subdivided on the basis of geomorphology and pervasive structure. The main units are dark and light materials. Dark materials are subdivided into dark grooved material (unit **dg**), dark lined material (unit **dl**), and dark furrowed material (unit **df**). Light materials are subdivided into light smooth material (unit **ls**), light grooved material (unit **lg**), and intermediate-albedo, mottled grooved material (unit **lmg**). Crater materials are classified as material of bright, fresh craters (unit **c<sub>3</sub>**), material of partly degraded craters (unit **c<sub>2</sub>**), material of degraded craters (unit **c<sub>1</sub>**), and palimpsest materials. The latter are high-albedo patches with subdued concentric ridges unit (**p<sub>3</sub>**) or material that lacks well-preserved structure (unit **p<sub>2</sub>**). No highly degraded palimpsests (unit **p<sub>1</sub>**) have been recognized in the Philus Sulcus area, although they are found in other quadrangles.

The west half of the quadrangle was imaged only at low resolution by Voyagers 1 and 2, and it is thus not geologically mappable using existing data. It contains largely light materials, a few small areas of dark materials, and some bright-rayed craters.

Of the mappable part of the quadrangle, containing about equal areas of light and dark materials, the southeastern area consists mostly of two large polygons of dark furrowed material, northern Marius Regio and the northern part of southern Marius Regio, separated by Mashu Sulcus. Three palimpsests 300 to 400 km in diameter are located in the southeasternmost area. The northeastern part of the quadrangle contains Ur Sulcus and Elam Sulci, several polygons of dark lined

material, and three areas of dark furrowed material. The southwestern part of the mapped area consists dominantly of light materials.

High-albedo, diffuse, bright materials are concentrated in the northern part of the quadrangle. This observation is consistent with the hypothesis that water-frost deposits are retained for longer periods of time in the cold environment of the northern latitudes (Squyres, 1980a). The diffuse deposits include both bright crater rays and part of the north polar frost cap, a continuous, diffuse, bright deposit lacking observable relief. The polar frost occurs north and west of northern Marius Regio; it may have accumulated by cold-trapping of water ice ablated by solar radiation (Purves and Pilcher, 1980) or by bombardment by the Jovian radiation belts (Johnson, 1985), or it may be a relict deposit formed at the time of emplacement of light materials (Shaya and Pilcher, 1984). The retention of albedo contrasts in spite of the polar frost suggests either that only a very thin frost layer is present or that frost is intermixed with and brightens the underlying regolith (Helfenstein, 1986, p. 305-309). Crater materials south of the frost-covered region are more commonly of low to intermediate albedo, probably because of greater frost ablation and formation of a silicate-enriched lag (Shoemaker and others, 1982).

### DARK MATERIALS

Dark materials as a whole are older than light materials, as evidenced by their higher crater density and superposition by light materials (Smith and others, 1979a, b). Dark materials occur in two modes: (1) as large polygons hundreds to thousands of kilometers across containing sets of subparallel to parallel furrows, exemplified by Galileo Regio and northern and southern Marius Regio; and (2) as smaller polygons 10 to 200 km across within large regions of light materials. In the smaller polygons, furrows are highly degraded and replaced by grooves or lineations.

Dark material in the large polygons is mapped as dark furrowed material (unit **df**). Furrows are linear, curvilinear, or wavy troughs 6 to 10 km wide, commonly having raised rims; they are typically 50 to a few hundred kilometers long. In the Philus Sulcus area they form three sets having parallel to subparallel orientations at a scale of hundreds of kilometers. The dominant set is composed of arcuate furrows (Smith and others, 1979a; Lucchitta, 1980; Shoemaker and others, 1982; Casacchia and Strom, 1984; Murchie and Head, 1987b). These furrows form a crudely concentric pattern on a hemispheric scale; they are commonly spaced 10 to 30 km apart in Marius Regio and about 50 km apart in Galileo Regio east of the map area. The concentric pattern and the location of a faint, giant palimpsestlike feature at the center of the pattern (to the southeast, outside the map area) suggest that the arcuate furrows originated as ring fractures due to an impact (McKinnon and Melosh, 1980; Shoemaker and others, 1982). However, the arcuate furrows also appear to have been modified by volcanism and extensional tectonism (Murchie and Head, 1987b). Alternatively, Casacchia and Strom (1984) suggested a purely tectonic origin for the arcuate furrows because of extension over a large mantle upwelling.

Two additional furrow sets are superposed on the arcuate furrows in Marius Regio. The first set is composed of furrows oriented approximately orthogonal to the arcuate furrows. The orthogonal furrows are widespread in Galileo Regio, east of the Philus Sulcus quadrangle, as narrow troughs 10 to 50 km long; some conspicuous furrows reach lengths of a few hundred kilometers (Casacchia and Strom, 1984). In Marius Regio, the orthogonal furrows occur as single troughs 50 to 150 km long that crosscut the arcuate furrows. The second superposed furrow set crosscuts the arcuate furrows at an oblique angle. These "oblique" furrows belong to a larger system arranged radially to a point near lat 22° S., long 135° (Murchie and Head, 1987b).

Furrow sets provide zones of weakness that have influenced linear boundaries of large polygons of dark furrowed material. These zones of weakness are both parallel and perpendicular to the furrows (Murchie and Head, 1985a, b), resulting in two pairs of zones of weakness. One pair is composed of the arcuate and orthogonal furrows. The other pair consists of the “oblique” furrows and furrows perpendicular to them. Although no furrows with this perpendicular orientation are found in the quadrangle, such furrows do occur in the southwestern part of the Galileo Regio quadrangle (Murchie and Head, 1987b).

Although furrows within each set are morphologically similar within Galileo Regio and also within Marius Regio, between the two regiones the furrows differ somewhat in morphology, age, and orientation. Both the arcuate and “oblique” furrows are shorter, less linear, and more closely spaced in Marius Regio. The orthogonal furrows in Marius Regio are consistently younger than the arcuate furrows, in contrast to their commonly greater relative age in Galileo Regio. The orientation of the arcuate furrows in the two regiones shifts abruptly by about 20° across Nippur Sulcus. The shift in furrow orientation as well as regional patterns of deformation in grooved materials suggest that the regiones were offset by shear contemporaneous with deformation of the oldest grooved materials (Murchie and Head, 1987a).

In their second mode of occurrence, dark materials form smaller polygons tens to hundreds of kilometers across, located north of and within Nippur Sulcus and west and south of Amon crater. In most of these polygons, as well as in the highly dissected western extremity of southern Marius Regio, furrows are degraded to shallow troughs or albedo lineaments in a sublinear to reticulate pattern. The material of these degraded polygons is mapped as dark lineated material (unit **dl**). Although some mottling by higher albedo patches occurs within many small dark polygons, the lineated material in the west margin of southern Marius Regio is characterized by a lower albedo than that of dark furrowed material immediately to the east. In addition, dark grooved material (unit **dg**) occurs at lat 57° N., long 215°, having a groove spacing of 20 to 30 km, and at lat 44° N., long 192°, having finer grooves with a 10-km spacing.

Although Ganymede may have been bombarded twice as heavily as Callisto by extra-Jovian objects (Passey and Shoemaker, 1982), crater density in Ganymede’s dark materials is about one-third of that on Callisto. This observation may be attributed to a longer time required for Ganymede to develop a lithosphere capable of supporting crater topography (Shoemaker and others, 1982) or to widespread early resurfacing (Smith and others, 1979a; Helfenstein, 1986, p. 310-313). The observation is consistent with Ganymede’s higher silicate content and radiogenic heat productivity.

## LIGHT MATERIALS

Light materials dominate the sulci that separate large polygons of dark furrowed material. Within the sulci are several small dark polygons that are partly covered by light material. Craters in light material that are believed to have penetrated to a depth of 1 km or more are interpreted to have excavated underlying dark material (Schenk and McKinnon, 1985). Also, crater density in light materials is substantially less than it is in dark materials. These observations suggest that light materials consist of a layer several hundred meters to 1 km or more thick that buries underlying, older, dark materials.

Smooth material (unit **ls**) embays topographic lows such as grooves and crater floors, suggesting that it was emplaced as a low-viscosity fluid, probably a silicate-poor brine or brine-ice slurry (Lucchitta, 1980). It occurs globally in three modes (Murchie and Head, 1985a), all of which are found in the Philus Sulcus area. The first mode is high-albedo deposits in the central parts of groove lanes, such as at lat

26° N., long 194° and lat 48° N., long 202°. The second mode is intermediate- to high-albedo, elongate to polygonal deposits, which are outlined and at places also dissected by throughgoing grooves or groove pairs; examples are at lat 50° N., long 190°; lat 23° N., long 205°; lat 23° N., long 232°; and lat 28° N., long 219°. The elongate, intermediate-albedo, smooth areas within Philus Sulcus may also be of this mode of occurrence. The third mode is diffuse-edged, intermediate-albedo deposits on margins of dark polygons adjacent to groove lanes, conspicuous grooves, or groove pairs. Such smooth material is found at lat 38° N., long 210° and lat 37° N., long 201°; at other locations it coalesces to form smooth polygons such as that at lat 33° N., long 188°. Images of this third mode show no protruding dark areas or gaps through which the smooth material apparently flowed, suggesting either blanketing by pyroclastic ice or flooding of low-lying dark materials.

Light materials that are pervasively grooved are mapped as grooved material (unit **lg**) or mottled grooved material (unit **lmg**). Grooves are linear to curvilinear troughs, U-shaped in cross section (Squyres, 1981). Grooved materials contain intersecting groove domains, and most have an intermediate to high albedo similar to that of smooth material. The dominance of troughs in grooved materials has led to the interpretation that they were formed by widespread extensional tectonism (Smith and others, 1979a, b; Lucchitta, 1980; Golombek and Allison, 1981; Shoemaker and others, 1982; Squyres, 1982; Bianchi and others, 1986; Murchie and others, 1986). Individual grooves may be degraded remnants of grabens or tension fractures; lithospheric thickness and strain rate probably controlled the exact mode of origin of these features (Parmentier and others, 1982; Squyres, 1982).

Orientations of groove sets are structurally controlled by the same two pairs of furrow-related zones of weakness that define the boundaries of large polygons of dark furrowed material (Murchie and Head, 1985a, b). Bianchi and others (1986) have shown in their measurements of groove orientation that the preferred orientation in this quadrangle is approximately parallel to the orthogonal and “oblique” furrows.

Domains having groove sets with these orientations dominate Elam Sulci and the southwestern part of the map area as well as Nippur, Mashu, and Anshar Sulci. Philus Sulcus and grooves in the southern part of Ur Sulcus are perpendicular to the “oblique” furrows. The dominant northwest orientation of groove lanes in this quadrangle is part of a larger global trend, in which most groove lanes and throughgoing grooves form low angles to small circles centered on a proposed paleopole of rotation near lat 70°-75° N., long 95° (Murchie and Head, 1986). This global pattern was proposed to result from structural control of groove-lane emplacement by relict tidal-despinning fractures that predated the furrows, combined with control by the possibly impact related furrows. Therefore, the dominant northwest groove-lane orientation in the Philus Sulcus area may have resulted from control by preexisting structures. Alternatively, Bianchi and others (1986) proposed that the dominant orientation results from stresses due to mantle convection.

The most conspicuous crosscutting relation of groove sets is the truncation of many of them against major groove lanes. Two examples of this relation are the contact of Nippur Sulcus with the groove domains to its north and the contact of Philus Sulcus with the grooves to its west. This relation appears to result from a confinement of groove-set propagation by older zones of weakness underlying the groove lanes (Golombek and Allison, 1981; Murchie and others, 1986). Despite the greater age of the zones of weakness than of the groove sets terminating against them, light materials within many of the groove lanes are superposed on the truncated groove sets. This relation is best seen at lat 45° N., long 195°, where the boundary of a groove set is only partly buried by light material in Nippur Sulcus.

Two additional classes of crosscutting relations of groove domains are particularly noteworthy. In the first class, groove lanes, throughgoing grooves, and groove pairs crosscut interior parts of other groove domains and segment them into smaller polygons. These relations are best seen where the north-trending groove lane centered at lat 45° N., long 183° crosscuts a wider northeast-trending groove lane, isolating its southwestern segment. In the second class, the groove set of a groove lane or grooved polygon terminates within a bounding groove lane. Examples are seen at the contact of the groove lanes at lat 51° N., long 201° and in southwestern Philus Sulcus. At lat 55° N., long 213°, the groove set from one grooved polygon is also superposed on the edge of another grooved polygon.

Clear evidence exists for temporal change in the regional orientation of groove sets. This change is seen north of Nippur Sulcus, where the oldest grooves (in Ur Sulcus) are oriented northeast. Crosscutting relations indicate that younger domains (in Elam and Nippur Sulci) are oriented progressively more northwest. A similar change in orientation is seen west of Philus Sulcus, which trends north-northeast. Grooves in the grooved polygon to the west, which are superposed on southwestern Philus Sulcus, have a northwest orientation; Mashu Sulcus, which crosscuts both features, is oriented west-northwest.

Lucchitta (1980) proposed that light grooved material develops in place from dark materials and that intermediate stages of conversion of the dark material may be found. Such intermediate stages occur in three areas within this quadrangle. The first area is at lat 33° N., long 190°, where conspicuous throughgoing grooves and groove pairs outline polygons 50 to 150 km long. Smooth material adjacent to the grooves has coalesced to completely cover one of the polygons, although the polygons to the north and south remain dark and their furrows are still resolvable. The second area is northwest of Anshar Sulcus, where narrow groove lanes and groove pairs outline small polygons of dark lineated material. Several of these groove lanes and groove pairs continue east of long 212°, within Anshar Sulcus, where the intervening polygons are light and smooth. Feather-edged margins of light material mark the transition from dark lineated material. Within Anshar Sulcus, the smooth polygons are of the same size and polygonal shape as the dark polygons to the northwest, and the intermediate area clearly consists of dark blocks partly covered by light material. The third transitional area is west of Anshar Sulcus (around lat 26° N., long 222°), where groove pairs and narrow groove lanes outline polygons of two size scales. Two large polygons, hundreds of kilometers across, are grooved and have an overall intermediate albedo and light mottling at a scale of tens of kilometers. These two polygons are mapped as mottled grooved material (unit **img**). The smaller polygons, tens to a few hundreds of kilometers across, are light and smooth, dark and lineated, or a mixture of the two types. The dark polygons are partly resurfaced by the coalescence of smooth deposits adjacent to the groove pairs and groove lanes.

Three consistent stratigraphic relations in these transitional areas suggest the sequence of events responsible for the conversion in place of dark furrowed to light grooved material: (1) the dissection of dark furrowed material into polygons by throughgoing grooves, groove pairs, or narrow groove lanes; (2) the coalescence of light smooth material adjacent to these grooves to partly or completely resurface the polygons; and (3) the superposition of grooves on the smooth deposits without attendant refilling. For the throughgoing grooves to be the sources of light smooth material and also to be superposed on it, emplacement of the material must have occurred between groove-forming events. Two additional observations on crosscutting relations of groove domains are useful in determining the sequence of events during grooved-terrain formation: Some groove sets are entirely confined within grooved polygons, apparently by older fracture zones, and some groove

lanes appear to have formed in preexisting zones of weakness outlining the polygons.

Based on the relations listed above, a sequence of events during grooved-terrain formation has been proposed and tested by detailed geologic mapping and crater-density measurements (Murchie and others, 1986). The sequence appears applicable to wide regions, including the Philus Sulcus area. First, dark furrowed material was dissected by throughgoing grooves or fracture zones to form polygonal blocks. Adjacent blocks were offset vertically, and smaller blocks were pervasively fractured to form lineated materials. Next, many downdropped blocks and areas adjacent to the throughgoing grooves were flooded by light smooth material, largely burying the throughgoing structures. Groove sets mostly confined to single polygons by their marginal fracture zones also developed at this time by intense fracturing, forming grooved polygons. Finally, newer grooves and groove lanes were superposed preferentially on the buried throughgoing zones.

### CRATER MATERIALS

As elsewhere on Ganymede, craters in the Philus Sulcus area belong to three geomorphic and albedo classes corresponding to degradational states. Craters consisting of fresh, high-albedo material (unit **c<sub>3</sub>**) have sharp rims, and many have preserved bright ejecta rays. The most conspicuous bright ejecta are associated with the craters Geb and Amon. Dark rays are uncommon; the only crater in light materials whose ejecta are completely dark is the **c<sub>3</sub>** crater at lat 23° N., long 236°. The high albedo of bright rays may result from small particle sizes of ray material, from condensation as frost of impact-generated water vapor, or from other processes (Chapman and McKinnon, 1986). The origin of dark rays is uncertain, but they may result in part from contamination of crater ejecta by fragments of impacting projectiles (Conca, 1981).

Partly degraded crater material (unit **c<sub>2</sub>**) has undergone only minor degradation of crater rims and ejecta, but it has an albedo close to that of background materials. Rays are not visibly associated with these **c<sub>2</sub>** craters; they apparently have ablated or been impact-gardened into the regolith (Shoemaker and others, 1982). Material of degraded craters (unit **c<sub>1</sub>**) is characterized by subdued rims, barely recognizable ejecta, flat floors, and low albedo close to that of the dark materials on which it occurs.

Palimpsests, the most degraded craters, are found in the southeastern part of the map area and are 300 to 450 km in diameter. Two palimpsests (unit **p<sub>2</sub>**) in dark furrowed material have an albedo slightly higher than that of target material and display partly to completely buried furrows. Because the furrows are not entirely buried in the distal parts of the palimpsests, the material there cannot be significantly thicker than the relief of the furrows, a few hundred meters or less (Shoemaker and others, 1982). The third palimpsest (unit **p<sub>3</sub>**) is on a contact between light and dark materials, has a higher albedo than does unit **p<sub>2</sub>**, possesses degraded remnants of basin rings, and is surrounded by a field of secondary craters. Palimpsests are interpreted to be craters whose high-relief features collapsed as a result either of low strength of the young lithosphere at the time of their formation or of viscous relaxation with time (Smith and others, 1979a, b; Parmentier and Head, 1981; Passey and Shoemaker, 1982).

Crater forms progress with size from simple bowl shapes to craters with central peaks, to craters with central pits, to multi-ringed basins (Passey and Shoemaker, 1982). A trend toward increasingly complex craters of the same size also exists in craters of greater ages. The latter progression probably occurs because, as Ganymede lost its internal heat and its early lithosphere thickened, craters of a given size formed with less complex morphologies and greater relief. Central-peak craters in the quadrangle range in size from 15 to 30 km, central-pit craters from less than

40 km to 120 km. The only basin having well-preserved rings, Geb, has an outer ring 120 km in diameter.

Rims of many craters are markedly polygonal to hexagonal; examples are at lat 37° N., long 181° and lat 24° N., long 195°. Generally, at least one linear rim segment or segments on opposite sides of the crater are parallel to the arcuate furrows, suggesting some structural control of crater shape by furrows.

Buried or highly degraded craters and craters that are crosscut by grooves are uncommon in light materials, but several buried craters are suggested by albedo curvilineaments or arcuate ridges having subdued relief. Examples are found at lat 58° N., long 207°; lat 44° N., long 185°; lat 23° N., long 194°; and lat 37° N., long 183°. At the resolution of Voyager images, it is difficult to be certain that these craters are buried and not in fact simply greatly flattened. Degraded or partly buried craters at lat 39° N., long 219° and lat 37° N., long 183° are in light materials but are crosscut by grooves, suggesting that a substantial period of time passed between resurfacing and the end of groove formation. The  $c_2$  craters at lat 24° N., long 195°; lat 63° N., long 192°; and lat 62° N., long 199° (Agrotos) are superposed partly on light material and partly on dark material, but no pronounced change in rim morphology is seen at the contacts, as might be the case if a large contrast existed in the viscosities of dark and light materials. No craters on dark materials are crosscut by arcuate furrows, but the degraded crater at lat 42° N., long 203° is crosscut by an “oblique” furrow.

## GEOLOGIC HISTORY

The first recognizable event in the Philus Sulcus area was the formation of a lithosphere, which is inferred to have been fractured by tidal despinning. Before any of the present surface features were formed, extensive resurfacing or viscous relaxation may have obliterated a Callisto-like crater population and formed dark-terrain surfaces. Subsequently, arcuate furrows formed as part of a hemispheric system, possibly by modification of ring fractures created by a giant impact. For some time impact craters were formed on the arcuate furrows and began to degrade because of mass wasting or viscous relaxation. Then widely spaced single furrows were superposed on the arcuate furrows in orthogonal and oblique directions. Crosscutting relations to the east in Galileo Regio (Casacchia and Strom, 1984) indicate that the “oblique” furrows were emplaced subsequent to the orthogonal ones. Cratering and degradation of high-relief features continued; the largest craters collapsed or viscously relaxed to leave little more than albedo patches as palimpsests.

In the map area, light grooved and smooth materials developed in place from dark furrowed material by a general three-stage process: (1) dissection of furrowed material into polygonal blocks, many of which developed lineated surfaces; (2) extensive resurfacing by silicate-poor brine or slush commonly followed by pervasive groove formation; and (3) superposition of throughgoing grooves and groove lanes. Contemporaneously with the earliest stages of groove formation, shear offset of large lithospheric blocks may have disrupted preexisting structures.

Crater formation continued, and by the end of light-material emplacement, the lithosphere had strengthened enough to support remnants of basin structures. What was a basin south of Nippur Sulcus did not collapse completely; its form is transitional between a basin and a palimpsest (Shoemaker and others, 1982). This structure was the last major impact feature in the quadrangle to be affected severely by palimpsest-formation processes. The last features to form were fresh craters, whose rays have not yet ablated or been impact-gardened into the regolith.

Ganymede's geologic history must be understood in terms of its thermal history and the development of its lithosphere. Five aspects of its thermal and lithospheric histories are particularly relevant. First, as Ganymede's internal temperature

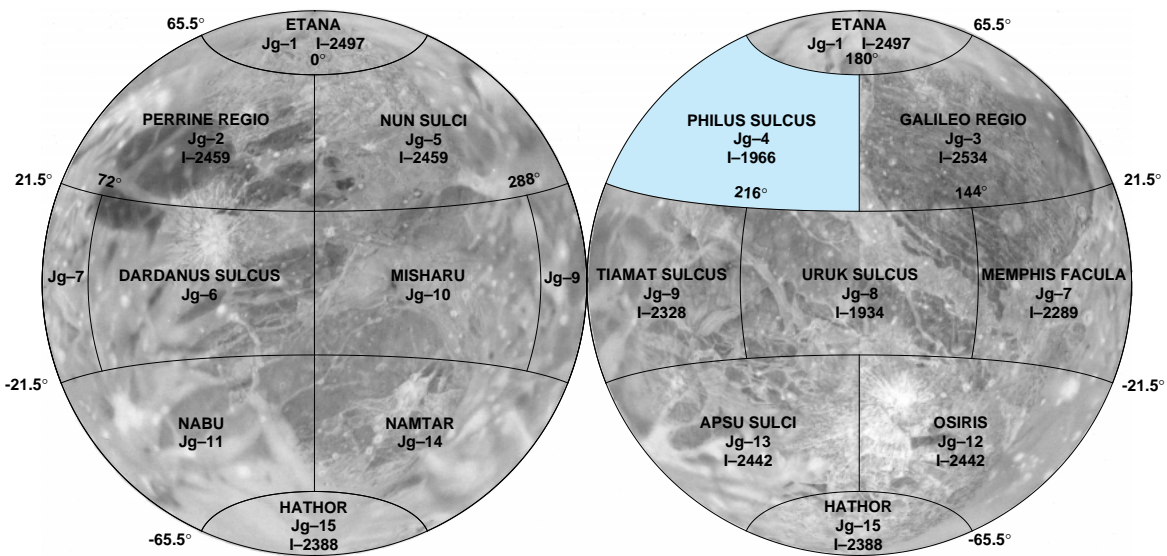
evolved, the thickness of the lithosphere changed in response to the evolving lithospheric thermal gradient (Consolmagno and Lewis, 1976; Parmentier and Head, 1979; Shoemaker and others, 1982). Lithospheric thickness, as estimated from studies of crater relaxation, increased from a few kilometers to 10 km at the time of furrow formation to 35 km at the time of groove formation. Alternatively, lithospheric thickness as estimated from the study of tectonic features may have decreased from 5 to 10 km during furrow formation to 2 to 5 km during groove formation (Golombek and Banerdt, 1986, 1987). Second, through the time of groove formation, the calculated Rayleigh number for the mantle is high enough that vigorous convection is assumed to have occurred, but it would have created only several bars or less of stress (Squyres and Croft, 1986). Third, several mechanisms may have caused a global volumetric increase that would have placed the entire lithosphere in tensional stresses tens to hundreds of bars in magnitude. Proposed mechanisms include thermal expansion (Zuber and Parmentier, 1984), differentiation (Squyres, 1980b), and mantle phase changes (Shoemaker and others, 1982). Fourth, early in the history of groove formation, stresses that may have been responsible for left-lateral offset of Galileo and Marius Regiones may have affected much of the quadrangle. Fifth, the formation of the basin Gilgamesh (Osiris quadrangle, centered at lat 59° S., long 124°), late in the history of groove formation, possibly reoriented Ganymede from a paleopole of rotation at lat 70°–75° N., long 95°. Distortion of the reorienting satellite would have created several bars of stress (Murchie and Head, 1986). Thickening of the lithosphere would have allowed crater forms of higher relief to have been supported, and it would have affected the style of fracturing and faulting due to tectonic activity (Squyres, 1982). Although global expansion possibly provided the dominant source of stress for groove formation, the resulting uniform tension would have added to the deviatoric stresses resulting from convection, global reorientation, and especially from large-scale shear. The summed stresses, acting upon relict zones of weakness (furrows and possibly tidal despinning fractures), may have created the regionally dominant groove orientations such as those seen in the Philus Sulcus area

#### REFERENCES CITED

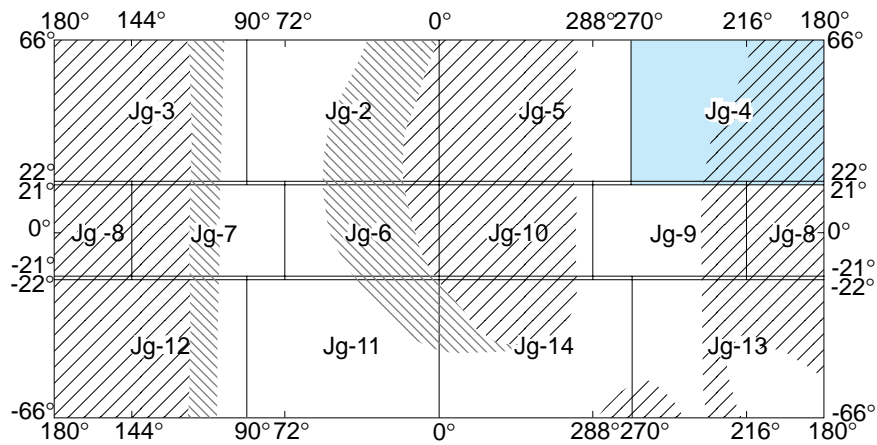
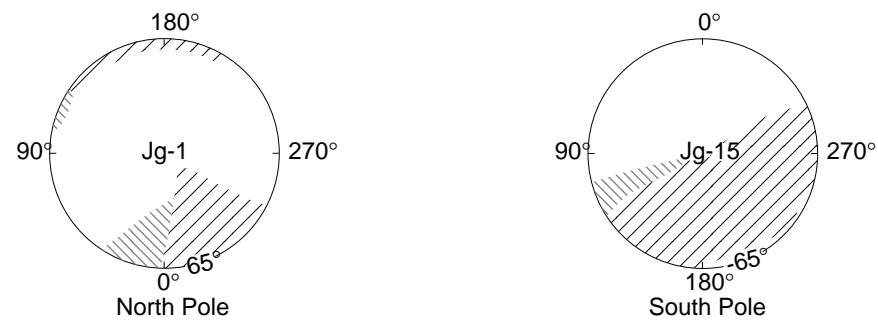
- Bianchi, Remo, Casacchia, Ruggero, Lanciano, Pasquale, Pozio, Stefania, and Strom, R.G., 1986, Tectonic framework of grooved terrain on Ganymede: *Icarus*, v. 67, p. 237–250.
- Casacchia, Ruggero, and Strom, R.G., 1984, Geologic evolution of Galileo Regio, Ganymede, *in* Lunar and Planetary Science Conference, 14th, Houston, 1983, Proceedings, part 2, *Journal of Geophysical Research*, v. 89, Supplement, p. B419–B428.
- Chapman, C.R., and McKinnon, W.B., 1986, Cratering of planetary satellites, *in* Burns, Joseph, and Matthews, Mildred, eds., *Satellites*: Tucson, University of Arizona Press, p. 492–580.
- Clark, R.N., Fanale, F.P., and Gaffey, M.J., 1986, Surface composition of natural satellites, *in* Burns, Joseph, and Matthews, Mildred, eds., *Satellites*: Tucson, University of Arizona Press, p. 437–491.
- Conca, James, 1981, Dark-ray craters on Ganymede: Lunar and Planetary Science Conference, 12th, Houston, 1981, Proceedings, p. 1599–1606.
- Consolmagno, G.J., and Lewis, J.S., 1976, Structural and thermal models of icy Galilean satellites, *in* Gehrels, Thomas, ed., *Jupiter*: Tucson, University of Arizona Press, p. 1035–1051.
- Golombek, M.P., and Allison, M.L., 1981, Sequential development of grooved terrain and polygons on Ganymede: *Geophysical Research Letters*, v.8, p.1139–1142.

- Golombek, M.P., and Banerdt, W.B., 1986, Early thermal profiles and lithospheric strength of Ganymede from extensional tectonic features: *Icarus*, v. 68, p. 252–265.
- \_\_\_\_\_, 1987, Early thermal profiles of Ganymede and Callisto, *in* Abstracts of Papers Submitted to the Eighteenth Lunar and Planetary Science Conference, Houston, 1987, p. 335–336.
- Helfenstein, Paul, 1986, Derivation and analysis of geologic constraints on the emplacement and evolution of terrains on Ganymede from applied differential photometry: Brown University, Ph. D. dissertation, 414 p.
- Johnson, R.E., 1985, Polar frost formation on Ganymede: *Icarus*, v. 62, p. 344–347.
- Lucchitta, B.K., 1980, Grooved terrain on Ganymede: *Icarus*, v. 44, p. 481–501.
- McKinnon, W.B., and Melosh, H.J., 1980, Evolution of planetary lithospheres: Evidence from multiringed structures on Ganymede and Callisto: *Icarus*, v.44, p. 454–471.
- Murchie, S.L., and Head, J.W., 1985a, Global tectonic mapping of Ganymede: A preliminary report, *in* Abstracts of Papers Submitted to the Sixteenth Lunar and Planetary Science Conference, Houston, 1985, p. 599–600.
- \_\_\_\_\_, 1985b, Tectonic features in the Jg-4 quadrangle of Ganymede, *in* Abstracts of Papers Submitted to the Sixteenth Lunar and Planetary Science Conference, Houston, 1985, p. 601–602.
- \_\_\_\_\_, 1986, Global reorientation and its effect on tectonic patterns on Ganymede: *Geophysical Research Letters*, v. 13, p. 345–348.
- \_\_\_\_\_, 1987a, Evidence for the existence of major shear zones on Ganymede, *in* Abstracts of Papers Submitted to the Eighteenth Lunar and Planetary Science Conference, Houston, 1987, p. 680–681.
- \_\_\_\_\_, 1987b, Origin and evolution of furrows in the dark terrain of Ganymede, *in* Abstracts of Papers Submitted to the Eighteenth Lunar and Planetary Science Conference, Houston, 1987, p. 682–683.
- Murchie, S.L., Head, J.W., Helfenstein, Paul, and Plescia, J.B., 1986, Terrain types and local scale stratigraphy of grooved terrain on Ganymede, *in* Lunar and Planetary Science Conference, 17th, Houston, 1986, Proceedings, part 1, *Journal of Geophysical Research*, v. 91, p. E222–E238.
- Parmentier, E.M., and Head, J.W., 1979, Internal processes affecting surfaces of low-density satellites: Ganymede and Callisto: *Journal of Geophysical Research*, v. 84, p. 6263–6276.
- \_\_\_\_\_, 1981, Viscous relaxation of impact craters in icy planetary surfaces: Determination of viscosity variation with depth: *Icarus*, v. 47, p. 100–111.
- Parmentier, E.M., Squyres, S.W., Head, J.W., and Allison, M.L., 1982, The tectonics of Ganymede: *Nature*, v. 295, p. 290–293.
- Passey, Q.R., and Shoemaker, E.M., 1982, Craters and basins on Ganymede and Callisto: Morphological indicators of crustal evolution, *in* Morrison, David, ed., *The satellites of Jupiter*: Tucson, University of Arizona Press, p. 379–434.
- Purves, N.G., and Pilcher, C.B., 1980, Thermal migration of water on the Galilean satellites: *Icarus*, v. 43, p. 51–55.
- Schenk, P.M., and McKinnon, W.B., 1985, Dark halo craters and the thickness of grooved terrain on Ganymede, *in* Lunar and Planetary Science Conference, 15th, Houston, 1985, Proceedings, part 2, *Journal of Geophysical Research*, v. 90, Supplement, p. C775–C783.
- Shaya, E.J., and Pilcher, C.B., 1984, Polar cap formation on Ganymede: *Icarus*, v.58, p. 74–80.

- Shoemaker, E.M., Lucchitta, B.K., Wilhelms, D.E., Plescia, J.B., and Squyres, S.W., 1982, The geology of Ganymede, *in* Morrison, David, ed., The satellites of Jupiter: Tucson, University of Arizona Press, p. 435–520.
- Smith, B.A., and the Voyager Imaging Team, 1979a, The Galilean satellites and Jupiter: Voyager 2 imaging science results: *Science*, v. 206, p. 927–950.
- \_\_\_\_\_, 1979b, The Jupiter system through the eyes of Voyager 1: *Science*, v. 204, p. 951–972.
- Squyres, S.W., 1980a, Surface temperatures and retention of H<sub>2</sub>O frost on Ganymede and Callisto: *Icarus*, v. 44, p. 502–510.
- \_\_\_\_\_, 1980b, Volume changes in Ganymede and Callisto and the origin of grooved terrain: *Geophysical Research Letters*, v. 7, p. 593–596.
- \_\_\_\_\_, 1981, The topography of Ganymede's grooved terrain: *Icarus*, v. 46, p. 156–168.
- \_\_\_\_\_, 1982, The evolution of tectonic features on Ganymede: *Icarus*, v. 52, p. 545–559.
- Squyres, S.W., and Croft, S.K., 1986, The tectonics of icy satellites, *in* Burns, Joseph, and Matthews, Mildred, eds., *Satellites*: Tucson, University of Arizona Press, p. 293–341.
- Zuber, M.T., and Parmentier, E.M., 1984, Lithospheric stresses due to radiogenic heating of an ice-silicate planetary body: Implications for Ganymede's tectonic evolution: *Journal of Geophysical Research*, v. 89, p. B429–B437.

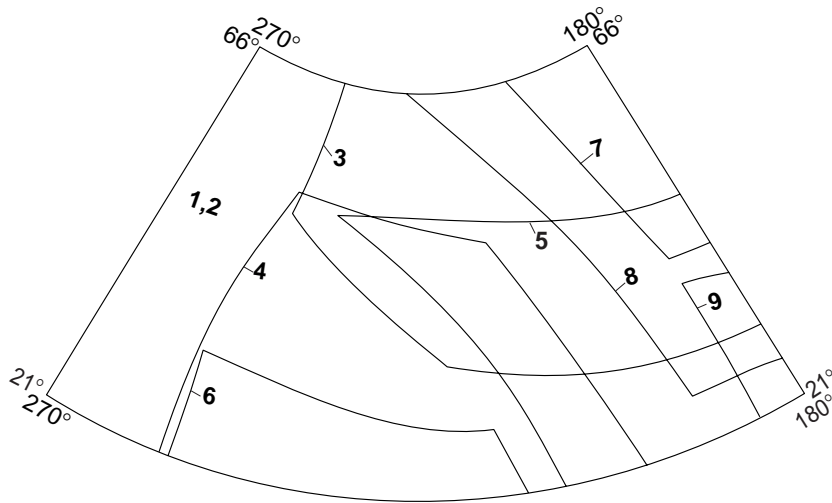


**QUADRANGLE LOCATION**  
 Number preceded by I refers to published geologic map



Approximate resolution of available Voyager images expressed as kilometers per picture element (pxl)





**INDEX OF MAPPING SOURCES**

The rendition of features on this map was controlled by reference to the primary source pictures outlined above. Supplemental source images used during the compilation are listed separately. Copies of various enhancements of these pictures are available from National Space Science Data Center, Code 601, Goddard Space Flight Center, Greenbelt, MD 20771.

**Primary Source**

VOYAGER 1		VOYAGER 2	
Index No.	Picture No.	Index No.	Picture No.
1	1207J1-004	3	0358J2-001
2	0786J1-002	4	0366J2-001
		5	0370J2-001
		6	0374J2-001
		7	0434J2-001
		8	0446J2-001
		9	0458J2-001

**Supplemental Source**

VOYAGER 1	Picture No.	VOYAGER 2	Picture No.
	0268J1-004		0809J2-003
	1211J1-004		0528J2-002
	1213J1-004		0092J2-001
	0015J1-003		0094J2-001
	0539J1-003		0096J2-001
	0318J1-002		0098J2-001
	0784J1-002		0100J2-001
	0788J1-002		0102J2-001
	0790J1-002		0104J2-001
			0350J2-001
			0352J2-001
			0354J2-001
			0362J2-001
			0380J2-001
			0384J2-001